Mon. Not. R. astr. Soc. (1981) **196**, 135–152

Fermi acceleration by relativistic shock waves

J. A. Peacock* *Mullard Radio Astronomy Observatory, Cavendish Laboratory, Madingley Road, Cambridge CB3 0HE*

Received 1980 November 6; in original form 1980 July 2

Summary. This paper discusses the acceleration of charged particles by astrophysical shock waves of arbitrary strength. As in the non-relativistic case, an energy spectrum of power-law form is produced, the slope of which varies according to the type of shock being considered. General solutions for the propagation of relativistic shock waves in a variety of physical conditions are presented, and the energy spectra for the resulting cosmic rays are derived. For strong shocks, a synchrotron spectral index in the range 0.3–0.5 is produced for propagation velocities less than $0.9c$; higher spectral indices can be produced only by weak shocks. The application of this acceleration mechanism to extragalactic radio sources is discussed briefly.

1 Introduction

Highly relativistic particles play a major role in astrophysics, being involved in the production of non-thermal continuum emission, the most common example of which is synchrotron radiation. The non-thermal sources often have radio or optical continuum spectra which are approximately of power-law form ($S \propto \nu^{-\alpha}$), indicating that the radiating electrons have a power-law integral energy distribution $N(>E) \propto E^{-x}$, where synchrotron theory gives the spectral index, α, as $x/2$. There are many deviations in detail from this simple form, but these may usually be accounted for by superposition of power laws of different slopes, and by allowing for the effects of self-absorption and of radiation losses on an energy spectrum initially of power-law form. In this paper, we shall consider principally the radio emission from extragalactic radio sources, although the analysis given below may be applied equally well to galactic radio sources or to optical emission. Indeed, the ranges of spectral indices found in non-thermal sources of all types are very similar; for the extragalactic sources, the observed range is $0.5 \lesssim \alpha \lesssim 2.0$, corresponding to $1 \lesssim x \lesssim 4$.

In addition, relativistic particles with energies up to $\sim 10^{20}$ eV are observed directly at the Earth as cosmic rays. These also have power-law energy distributions, with $x \simeq 1.5$. For many years there was no satisfactory explanation of these results. The high energies in

* Present address: Royal Observatory, Blackford Hill, Edinburgh EH9 3HJ, Scotland.

themselves were no problem, and many mechanisms involving turbulence or electromagnetic waves in plasmas were advanced (for a review of such mechanisms, see Parker 1976); the difficulty lay in obtaining a power-law of the observed slope without assuming physical conditions unlikely to be encountered in practice. Recently, however, it has been shown (Axford, Leer & Skadron 1977; Bell 1978a; Blandford & Ostriker 1978) that Fermi acceleration in a shock front can produce a power-law distribution with a slope close to that observed.

The basis of the acceleration mechanism lies in recognizing that astrophysical plasmas are collisionless, implying that the disordering which occurs in the shock front must be achieved via turbulent electromagnetic fields. This being so, an energetic particle may have a sufficiently high mass-to-charge ratio to penetrate the shock front undeviated. Now, if there exists some mechanism whereby these particles undergo pitch angle scattering in the rest frames of the fluid on each side of the shock, then they may cross and re-cross the shock and undergo acceleration. This scattering process may be attributed to a variety of mechanisms, the simplest of which is scattering by magnetic irregularities. Bell (1978a) also considers the possibility that particles moving parallel to an ordered magnetic field can generate Alfvén waves, which then lead to scattering. This process is an unstable one in which the momentum change of a particle that undergoes scattering generates a new Alfvén wave, which can then sustain the scattering. In this picture, the scattering is not strictly isotropic in the fluid rest frame, but since the mechanism is effective only when $u_{\rm shock} \gg u_{\rm Alfén}$, the difference is not significant. Bell (1978a) then shows that, for a strong shock propagating into a cold fluid, an initial distribution of suprathermal particles will be accelerated so as to have an energy distribution $N(>E) \propto 1/E$, corresponding to a spectral index of 0.5. These ideas have been applied, with some success, to the production of galactic cosmic rays via the shock waves generated by supernovae (Bell 1978b; Blandford & Ostriker 1980).

The work described in this paper was motivated by the desire to study also particle acceleration in the powerful extragalactic sources. The previous analysis is not directly applicable to such objects, as the shock fronts present in them are likely to move at large fractions of the speed of light. In compact sources of scale ~ 10 pc, apparent superluminal motions, very fast variability and one-sided 'jets' have established the case for bulk motions with a Lorentz factor $\gamma \sim 5$ (Scheuer & Readhead 1979). In the beam model of double radio sources (Blandford & Rees 1974), this would correspond also to the velocity of material in the beams of plasma which supply energy to the extended outer lobes. These outer lobes may also involve large velocities: Longair & Riley (1979) have analysed the asymmetry of double radio sources and derived an upper limit of $0.25\,c$ for the velocity of advance of the hot-spots at the outer edges of the extended lobes. If we wish to study particle acceleration in such sources, it is therefore necessary to consider shocks with propagation velocities arbitrarily close to c.

Section 2 of this paper presents the analysis of particle acceleration for a relativistic shock. Section 3 considers the propagation of relativistic shocks in detail and derives the particle spectra produced for a variety of physical conditions. Finally, possible modifications to the basic mechanism and its application in practice are discussed in Section 4.

2 The acceleration mechanism

2.1 OUTLINE OF THE PROBLEM

Fig. 1 shows the simple two-dimensional shock geometry to be considered, in the frame in which the shock front is stationary. u_1 and u_2 are the velocities of the bulk fluid upstream and downstream. Quantities pertaining to the suprathermal particles undergoing acceleration

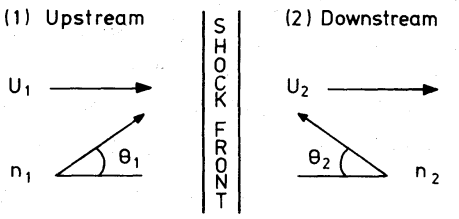

Figure 1. The simple plane-shock geometry to be considered, viewed in the frame in which the shock front is stationary. The bulk flow velocities upstream and downstream are u_1 and u_2. The proper number densities of suprathermal particles upstream and downstream are n_1 and n_2. The crossing angles θ_1 and θ_2 are defined in the rest frame of the bulk fluid.

are all measured in the rest frame of the fluid on either side, so that n_1 and n_2 are the proper number densities of relativistic particles.

The acceleration process which we wish to study consists of suprathermal particles crossing and re-crossing the shock front and gaining energy via the velocity difference of the bulk flows on either side. We shall analyse this process via the single-particle approach of Bell (1978a), rather than the fluid-dynamical methods of Axford *et al.* (1977) or Blandford & Ostriker (1978). In common with all these authors, we consider only the situation where the suprathermal particles are assumed to have a negligible effect on the propagation of the shock wave in the bulk material.

Consider N_0 particles crossing from the upstream region to the downstream region, each with initial energy E_0. There will be a probability $P(\theta_1)$ that a particle will eventually return and, if it does so, its energy will be increased by some factor $\delta(\theta_1, \theta_2)$, where θ_1 and θ_2 are the angles of crossing and re-crossing the shock (see Fig. 1). In principle, P and δ as defined above might be expected to be functions of E_0, but in fact both are energy-independent (see Sections 2.3 and 2.4). After k cycles of crossing and re-crossing, we shall have N of the N_0 particles remaining on the upstream side, where

$$\frac{N}{N_0} = \langle P \rangle^k \tag{1}$$

and $\langle P \rangle$ is $P(\theta_1)$ averaged over the numbers of particles crossing with various values of θ_1. Each of the particles remaining will have a different energy E, depending on its exact values of θ_1 and θ_2 for each crossing, such that

$$\ln\left(\frac{E}{E_0}\right) = \sum_{i=1}^{k} \ln(\delta_i). \tag{2}$$

Hence, after each crossing, the distribution of energies is broadened but shifted to higher energy. Now the central limit theorem tells us that, in the log plane, the distribution of energies quickly becomes Gaussian, so the median energy, E_m, is given by

$$\ln\left(\frac{E_m}{E_0}\right) = k \langle \ln \delta \rangle, \tag{3}$$

where $\langle \ln\delta \rangle$ is $\ln\delta$ averaged over the numbers of particles returning at θ_2, having crossed at θ_1. This is not the same as averaging over the numbers of particles crossing at θ_1 and recrossing at θ_2 separately, since $P(\theta_1)$ must be incorporated. The energy distribution produced by the injection of particles at E_0 therefore consists, in the log plane, of a series of Gaussians equally spaced by $\langle \ln\delta \rangle$, each successive distribution being broader and containing fewer particles

than the previous one. Hence, if we convolve this distribution with a distribution of E_0 which is wider in the log plane than $\langle \ln\delta \rangle$, then the result is the same as if we had ignored the broadening of the Gaussians and had taken each particle to have its energy increased by the same factor, $\exp(\langle \ln\delta \rangle)$, at each crossing. Hence, from equations (1) and (3), the integral energy spectrum is given by

$$\frac{N}{N_0} \propto \left(\frac{E}{E_0}\right)^x , \tag{4}$$

where

$$x = \frac{\ln(\langle P \rangle)}{\langle \ln\delta \rangle} . \tag{5}$$

2.2 THE DISTRIBUTIONS OF θ_1 AND θ_2

In this Section, and in those that follow, we use units such that $c = 1$.

The argument in the previous section leaves unspecified the distributions of θ_1 and θ_2 appropriate for performing the averaging in equation (5). The tacit assumption is that, after several crossings, the distributions of θ_1 and θ_2 will tend to a form determined merely by the nature of the scattering process on either side of the shock. Rather than attempting to follow this process in detail, we instead consider a simple situation where the distribution of suprathermal particles about the shock front is in a steady state. In this case, the angular distributions required in equation (5) should be given simply by the numbers of particles that cross the shock at θ_1 and θ_2 in equilibrium. However, the determination of this steady-state distribution is complicated by the fact that, since there will be a net drift of particles downstream, injection of particles is required to maintain the equilibrium state. These injected particles will be created with some angular distribution which could affect the distributions of θ_1 and θ_2 for particles that cross the shock. To tackle this problem, we note that any specific assumptions we make about the nature of the injection should not affect the general answer which we are attempting to obtain; this must depend only on u_1 and u_2 and on the nature of the scattering around the shock. Therefore, let us assume that any injection is confined to the region of the shock front itself: in this case, the angular distributions of particles at large distances away from the shock upstream and downstream will be unaffected by the injection. To calculate these distributions, we must consider in more detail the spatial variations in the number density of suprathermal particles about the shock front.

For shocks with $u_1 \ll 1$, the diffusion equation applies and the steady-state number density of suprathermal particles of a particular energy is given by Bell (1978a) as

$$n_1 = A + B\exp\left(-\int_0^x \frac{u_1}{D(x')}\,dx'\right) \qquad (x > 0), \tag{6}$$

$$n_2 = C \qquad (x < 0), \tag{7}$$

where x is the distance from the shock front (defined so that x increases in the upstream direction) and D is the diffusion coefficient. Thus the density of particles is constant behind the shock, but decreases ahead of it. In the expression for n_1, the first term represents pre-existing particles in the upstream medium, whereas the second represents the diffusion ahead of the shock of the particles that have crossed from the downstream side. When u_1 becomes relativistic, the diffusion equation no longer applies and the above expressions for n_1 and

n_2 require modification. However, the basic situation remains unaltered: the requirement of time independence means that n_2 still remains a constant and n_1 will still decrease ahead of the shock. Hence, since isotropic scattering is assumed to occur in the rest frames of the upstream and downstream fluids, the angular distribution of the suprathermal particles downstream of the shock must become isotropic in the rest frame of the downstream flow. Due to the spatial variation of n_1, however, the situation upstream is more complex; in order to obtain an expression for the distribution of θ_1, we must consider a specific model for the scattering process. For simplicity, we shall assume that the scattering is due to pre-existing magnetic irregularities in the upstream medium. This is not by any means the only possibility, but should give us a useful guide to the sort of anisotropies that may exist in the upstream θ_1 distributions. For this calculation, it is most convenient to work in the shock frame; consider a particle travelling at an angle ϕ to the shock normal, where $\phi = 0$ is defined to be in the downstream direction. Thus, on the upstream side

$$\cos\phi = \frac{\cos\theta_1 + u_1}{1 + u_1\cos\theta_1}\,, \tag{8}$$

whereas on the downstream side

$$\cos\phi = -\frac{\cos\theta_2 - u_2}{1 - u_2\cos\theta_2}\,. \tag{9}$$

The number of particles travelling in the range ϕ to $\phi + d\phi$, dn, is determined by the sum of the scattered contributions from other regions of the upstream fluid. If we evaluate dn by summing the contributions received at a point which is a distance x ahead of the shock as measured in the shock frame, then we may write

$$dn \propto F(\phi)\int_0^\infty n_1(x + r\cos\phi)\,P(r)\,dr\,, \tag{10}$$

where $F(\phi)$ is an angular factor depending on the anisotropy of the scattering, r is the distance from the point considered as measured in the shock frame, and $P(r)$ is the probability that a particle will travel a distance r in the shock frame without being scattered. Since the scattering is isotropic in the fluid rest frame, $F(\phi)$ is simply proportional to $d(\cos\theta_1)$, where

$$d(\cos\theta_1) = \frac{d\cos\phi}{\gamma_1^2(1 - u_1\cos\phi)^2}\,. \tag{11}$$

An equation such as (10) may always be satisfied by a self-similar exponential solution for $n_1 : n_1 \propto \exp(-kx)$, hence

$$n_1(x + r\cos\phi) \propto \exp(-kr\cos\phi)\,. \tag{12}$$

Finally, the form of $P(r)$ depends on the assumed distribution of mean free paths, which depends in turn on the exact distribution of magnetic irregularities considered. For simplicity, we shall consider the distribution of mean free paths, $g(\lambda)$, in the fluid frame to have the form appropriate for a constant scattering probability per unit time

$$g(\lambda) = \frac{1}{\lambda_0}\exp(-\lambda/\lambda_0)\,, \tag{13}$$

from which it follows that

$$P(r) = \exp(-\gamma_1 r(1 - u_1\cos\phi)/\lambda_0)\,. \tag{14}$$

Although this model for the scattering process is a highly idealized one, it should be sufficient to yield some insight into the type of anisotropy that may exist in the upstream angular distributions. As discussed in Section 3.3, the spectral indices predicted by this analysis do not in fact depend strongly on the precise form of these distributions.

When the above assumptions are made, the angular dependence of $d\Phi_1$, the flux per unit area of particles travelling at ϕ in the upstream region, is given by equation (10) as

$$d\Phi_1 \propto \frac{\cos\phi\, d(\cos\phi)}{(1-u_1\cos\phi)^2(1+a\cos\phi)}, \tag{15}$$

where

$$a = \frac{k\lambda_0}{\gamma_1} - u_1 .$$

The parameter a (and hence k) is determined by the condition that the net flux of particle number measured in the shock frame should be zero for a steady-state solution. Hence

$$\int_{-1}^{1} d\Phi_1 = 0 ,$$

which yields

$$\ln\left[\frac{(1-u_1)(1-a)}{(1+u_1)(1+a)}\right] + \frac{2(u_1+a)}{(1-u_1^2)} = 0 . \tag{16}$$

For small u_1, $a \simeq 2u_1$; for large u_1, a tends to 1.

By a similar argument, we may also obtain the flux of particle number per unit area downstream of the shock, $d\Phi_2$, as

$$d\Phi_2 \propto \frac{\cos\phi\, d(\cos\phi)}{(1-u_2\cos\phi)^3} . \tag{17}$$

This form is in fact independent of the model of the scattering adopted, being merely the result of transforming the isotropic distribution that exists in the downstream rest frame.

Now, having found the distributions of ϕ in the upstream and downstream regions, we must consider how these are related to the distributions of ϕ crossing the shock. The problem is that, within one mean free path on either side of the shock, the distributions given by equations (15) and (17) begin to be affected by the contributions of the particles that have crossed the shock. Hence, the actual distribution of ϕ for particles crossing the shock will be some form intermediate between equations (15) and (17). This fact is sufficient to allow reasonable limits to be put on the variation of α due to the uncertainty in the distribution of ϕ at the shock (see Section 3.3), and we shall not attempt a precise solution of this problem.

2.3 CALCULATION OF $\delta(\theta_1, \theta_2)$

Consider a particle with energy E crossing the shock at θ_1, being scattered in pitch angle (but gaining no energy) in the rest frame of the downstream fluid, and returning at θ_2. Its energy after this process is given by a double Lorentz transformation

$$E' = E\gamma_\Delta^2(1+\Delta\cos\theta_1)(1+\Delta\cos\theta_2), \tag{18}$$

where

$$\Delta \left(= \frac{u_1 - u_2}{1 - u_1 u_2} \right)$$

is the velocity difference of the upstream and downstream flows. Hence

$$\langle \ln \delta \rangle = 2 \ln \gamma_\Delta + \langle \ln (1 + \Delta \cos \theta_1) \rangle + \langle \ln (1 + \Delta \cos \theta_2) \rangle , \tag{19}$$

where

$$\langle \ln (1 + \Delta \cos \theta_1) \rangle = \frac{\int_0^1 P(\theta_1) \ln (1 + \Delta \cos \theta_1) \, d\Phi_1}{\int_0^1 P(\theta_1) \, d\Phi_1} , \tag{20}$$

$$\langle \ln (1 + \Delta \cos \theta_2) \rangle = \frac{\int_{-1}^0 \ln (1 + \Delta \cos \theta_2) \, d\Phi_2}{\int_{-1}^0 d\Phi_2} . \tag{21}$$

In these expressions, $d\Phi_1$ and $d\Phi_2$ represent the actual numbers of particles crossing the shock at θ_1 and θ_2 respectively. Equation (20) is simpler than (21), as $d\Phi_2$ gives the probability of returning at θ_2 directly.

2.4 CALCULATION OF $P(\theta_1)$

$P(\theta_1)$ must be determined by the scattering in the downstream region. This is characterized by a mean free path λ, which will in general be a function of energy. Since $P(\theta_1)$ can depend on u_1, u_2, λ and θ_1 only, we see by a dimensional argument that $P(\theta_1)$ must be independent of λ, and hence of energy. This argument will break down only when λ becomes comparable with the scale of the accelerating region, and this will determine a high energy cut-off.

To obtain an expression for $P(\theta_1)$, we adopt a simple model for the post-shock scattering process. Let a particle possess a mean free path, λ, in the fluid frame, such that the particle travels a distance λ and is then isotropized. If the particle crosses the shock at θ_1, it travels at an angle ϕ to the shock normal in the shock frame, where

$$\cos \phi = \frac{\cos \theta_1 + u_1}{1 + u_1 \cos \theta_1} . \tag{22}$$

The particle is first scattered when it is a distance b from the shock as measured in the downstream rest frame, where

$$b = \frac{\lambda \cos \phi}{\gamma_2^2 (1 - u_2 \cos \phi)} . \tag{23}$$

The problem now becomes a standard one in probability theory: the random walk with a moving barrier. This may be solved by means of the diffusion equation (see Cox & Miller 1965). Although the diffusion approximation is not strictly valid in this case, the answer obtained should still be useful since (i) u_2 is generally less than 1/3 (see Section 3.3), and

(ii) many particles will take a large number of scatterings to cross the shock. In this approximation, we have for the probability of return as a function of b,

$$P(b) = A \exp(-u_2 b/D), \tag{24}$$

where D is the diffusion coefficient and A is an arbitrary constant. Finally, we must average b over a distribution of mean free paths: we again take this to have the simple form of equation (13). In this case, since we have $D = \lambda_0/3$, we obtain

$$P(\phi) = A\left[1 + \frac{3u_2\cos\phi}{\gamma_2^2(1-u_2\cos\phi)}\right]^{-1}. \tag{25}$$

The above analysis leaves the constant A undetermined; to overcome this problem, we can use a direct argument to find $\langle P\rangle$ for one particular distribution of ϕ. If we require the distribution of ϕ for particles crossing from upstream to downstream to be the same as the form at large distances downstream (equation 17), then this distribution of ϕ will apply throughout the downstream region. Hence, $P(\phi)$ averaged over equation (17) will be given simply by the ratio of the flux of particle number crossing from downstream to upstream to the flux crossing from upstream to downstream. Therefore, from (17), we have in this case

$$\langle P\rangle = \frac{-\int_{-1}^{0} \frac{\cos\phi\, d(\cos\phi)}{(1-u_2\cos\phi)^3}}{\int_{0}^{1} \frac{\cos\phi\, d(\cos\phi)}{(1-u_2\cos\phi)^3}} = \left(\frac{1-u_2}{1+u_2}\right)^2, \tag{26}$$

which allows the constant A to be found for a given value of u_2.

Since, for strong shocks, $u_2 < 1/3$ (see Section 3.3), the expression for $P(\phi)$ in (25) should be quite accurate. Before proceeding further, it is nevertheless advisable to check this. As a test, therefore, we evaluated $P(\phi)$ numerically by following the scattering process step-by-step. If the above assumptions about the nature of the post-shock scattering and the distribution of mean free paths are made, then it is possible to simulate the random walk and find the probability of return as a function of the point at which the particle is first scattered. Using (13), we can then average this probability over the distribution of mean free paths to find $P(\phi)$. We chose to perform this simulation for the case $u_2 = 1/3$, to provide the most severe test of equation (25). The resulting form for $P(\phi)$ is shown in Fig. 2, together with the curve derived from (25) and (26). We see that, even in this extreme limit of post-shock velocity, the analytical expression gives a result quite close to that of the numerical simulation. For $\cos\phi > 0.5$, there is little difference between the two curves and both predict that the minimum value of $P(\phi)$ should be about 0.2. Equation (26) shows that, for $u_2 = 1/3$, $P(\phi)$ averaged over the distribution in (17) should be 0.25; this was found to be the case for our numerical simulation, giving confidence that it had been performed correctly. Although these calculations have been based on a specific model for the downstream scattering, the following points suggest that the results are likely to be model-independent. Since the averaging of $P(\phi)$ based on (17) is quite strongly biased towards $\cos\phi \simeq 1$ for $u_2 = 1/3$, it is clear that $P(\phi)$ for $\cos\phi = 1$ must be close to 0.25, independent of the exact nature of the downstream scattering. This fact, combined with the requirement that $P(\phi)$ must be less than 1 for $\cos\phi = 0$, suggests that any form for $P(\phi)$ that is to be consistent with $\langle P\rangle = 0.25$ must be quite similar to the curves in Fig. 2. In view of these points and of the good agreement between the analytical expression for $P(\phi)$ and the numerical simulation, we are

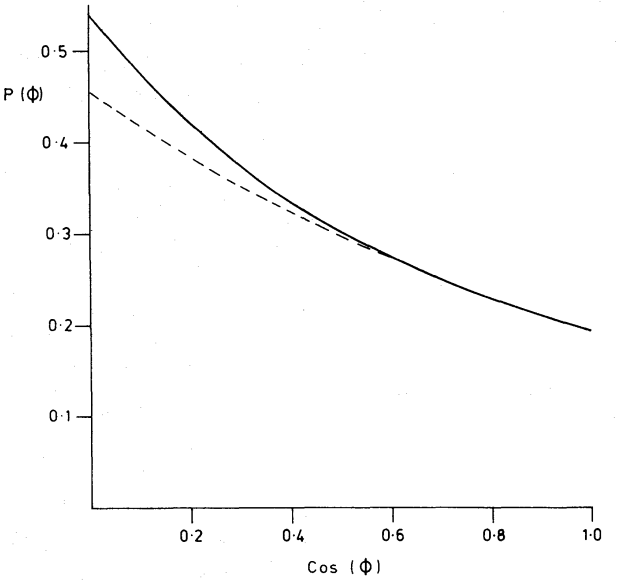

Figure 2. The probability of return as a function of crossing angle as measured in the shock frame, $P(\phi)$, for $u_2 = 1/3$. The solid line is the result of the numerical simulation, and the dashed line shows the prediction of equations (25) and (26).

confident that the use of equations (25) and (26) for $P(\phi)$ will not produce any important errors in α.

Thus, we now have an expression for $P(\phi)$ and also reasonable limits within which the distributions of θ_1 and θ_2 for particles crossing the shock must lie. Hence, given u_1 and u_2, we are in a position to evaluate the integrals in (20) and (21) numerically and find α.

3 The propagation of relativistic shock waves

3.1 THE SHOCK EQUATIONS

The fundamentals of relativistic shocks are given by Landau & Lifshitz (1959) and we shall use their notation here. There are three jump conditions

$$\gamma_1^2 u_1 w_1 = \gamma_2^2 u_2 w_2 , \tag{27}$$

$$\gamma_1^2 u_1^2 w_1 + P_1 = \gamma_2^2 u_2^2 w_2 + P_2 , \tag{28}$$

$$\gamma_1 u_1 \rho_1 = \gamma_2 u_2 \rho_2 , \tag{29}$$

where e = energy density, P = pressure, w = enthalpy = $e + \rho$ and ρ = rest mass density of the bulk fluid. Additionally, we require an equation of state for the bulk fluid and, following Blandford & McKee (1976), we consider:

$$P = (\Gamma - 1)(e - \rho) , \tag{30}$$

where Γ is a parameter which varies between 5/3 for cold material and 4/3 for material which is sufficiently hot for its internal motions to be relativistic. In these two limits, Γ is precisely the ratio of specific heats, but not for intermediate cases. In general, the processing of the bulk fluid by the shock will change the thermodynamic state so that Γ has different values in the pre-shock and post-shock regions. This is considered in Section 3.2. Since Γ varies, (30) is not precisely an equation of state: it merely allows us to eliminate ρ in terms of Γ.

The solution of (27)–(29) to find the relation between u_1 and u_2 is simplified in two cases:

(a) $\Gamma_1 = \Gamma_2 = 4/3$.

This is a shock wave propagating in a relativistic gas. Equations (34) and (35) yield

$$3u_1 + 1/u_1 = 3u_2 + 1/u_2, \tag{31}$$

which gives u_2 as a function of u_1 directly.

(b) Strong shocks.

In this case, $P_2/\rho_2 \gg P_1/\rho_1$, which is always true for a shock propagating into cold material. Blandford & McKee give

$$R_2 \equiv e_2/\rho_2 = \gamma_\Delta w_1/\rho_1, \tag{32}$$

$$\gamma_1^2 = \frac{(\gamma_\Delta + 1)(\Gamma_2(\gamma_\Delta - 1) + 1)^2}{\Gamma_2(2 - \Gamma_2)(\gamma_\Delta - 1) + 2}, \tag{33}$$

where R is the mean internal Lorentz factor of the bulk material. Additionally, we may derive

$$\gamma_2 = \frac{\gamma_1}{\Gamma_2(\gamma_\Delta - 1) + 1}. \tag{34}$$

Since we may find u_1 and u_2 as a function of the single parameter R_2 if we know Γ_2, the general equation of state which we require in order to express u_1 and u_2 in terms of a single parameter is $\Gamma(R)$.

For material with Γ_1 between 5/3 and 4/3, there is no analytic solution and (27)–(29) must be solved numerically. This may be done if the ratios w_1/ρ_1, w_2/ρ_2, w_1/P_1 and w_2/P_2 are known; again we require the equation of state $\Gamma(R)$ if the solution for u_1 and u_2 is to be parameterized in terms of R_2 for a given initial value of Γ_1.

3.2 THE EQUATION OF STATE

The natural assumption in deriving an equation of state is that of thermal equilibrium. In the absence of two-body processes in a collisionless plasma, this may not be achieved easily, but may be valid for the unshocked material. The basic thermodynamics of relativistic gases are given by Chandrasekhar (1939). For a single-particle gas at temperature T, we have

$$P = \frac{\rho kT}{m}, \tag{35}$$

$$R \equiv e/\rho = \frac{3}{z} + \frac{K_1(z)}{K_0(z) + 2K_1(z)/z}, \tag{36}$$

where $z = m/kT$ and K_0 and K_1 are modified Bessel functions (see Abramowitz & Stegun 1965). The appropriate relations for an astrophysical plasma (with 25 per cent of helium by mass) may be derived simply from these by summing over all species of particles as follows:

$$P = \sum_i \frac{\rho_i kT}{m_i}, \tag{37}$$

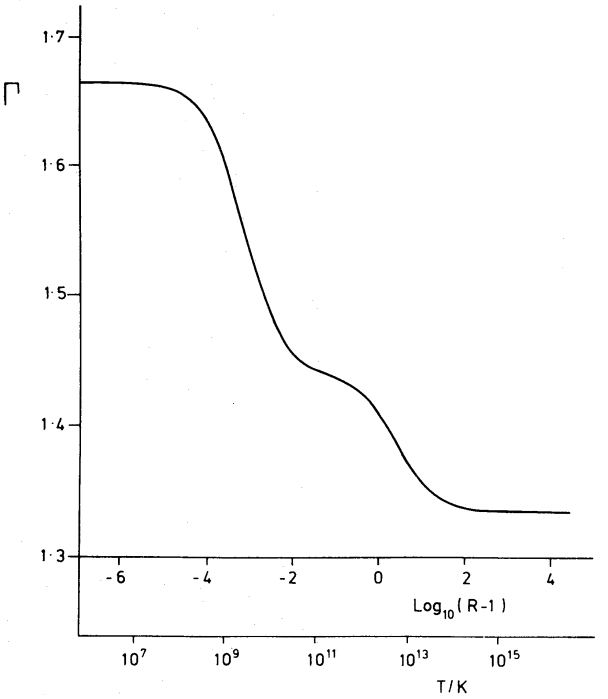

Figure 3. The equation of state $\Gamma(R)$ for an astrophysical plasma in thermal equilibrium. The temperature scale which corresponds to the scale of R in this case is also shown.

$$e = \sum_i R_i \rho_i \,, \tag{38}$$

$$\rho = \sum_i \rho_i \,. \tag{39}$$

This allows us to derive the $\Gamma - R$ relation (Fig. 3), and hence all ratios required for a solution of the shock equations. This $\Gamma - R$ curve gives the value $\Gamma = 5/3$ up to temperatures $\sim 10^9$ K, beyond which point Γ falls rapidly – levelling off at $\Gamma \simeq 1.45$ at a temperature of $\sim 10^{10}$ K before dropping rapidly again to $\Gamma = 4/3$. This first rapid fall is caused by the electrons becoming relativistic while the H and He nuclei are still moving sub-relativistically. The worrying feature of this solution is that the electrons are required to move so much faster than the protons (which do not become relativistic until the electrons have Lorentz factors ~ 1000). In a normal gas, this would be achieved by two-body collisions leading to equipartition of energy. Since the plasmas we consider here are collisionless, thermalization may not take place and we thus need to consider the difference this will make to shock propagation.

An extreme alternative to thermalization may be visualized in terms of a shock front which consists only of magnetic irregularities and therefore preserves, in its own frame, the energies of incoming particles. In this case, using the same θ_1 and θ_2 as in Fig. 1, but now considering bulk particles,

$$\gamma_1(E_1 + u_1\pi_1\cos\theta_1) = \gamma_2(E_2 - u_2\pi_2\cos\theta_2)\,, \tag{40}$$

where π_1 and π_2 are the momenta of the bulk particles in the upstream and downstream rest frames. The energies of all bulk particles are thus increased by a mean factor of about γ_1/γ_2. For a simple model of the effect of this on an incoming gas, let us assume that the shock takes all incoming particles and raises their energies by the same factor β (not to be confused

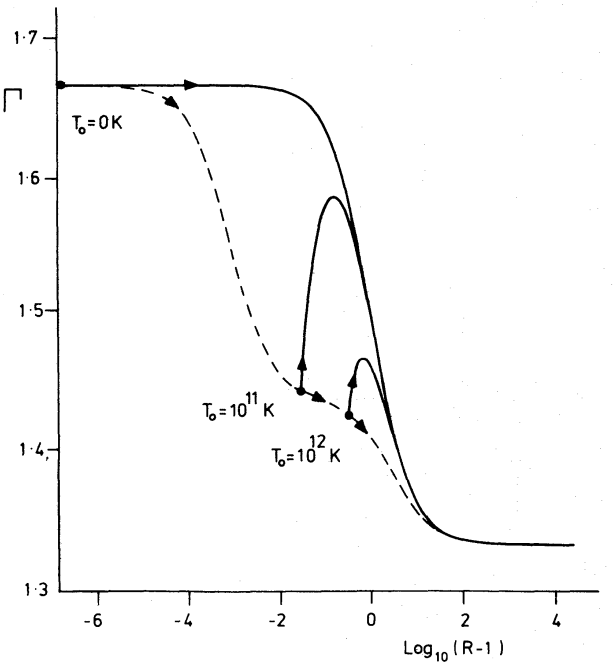

Figure 4. Possible thermodynamic histories for the shocked material, illustrated for three initial temperatures of the unshocked material: 0, 10^{11} and 10^{12}K. From each of these starting points, two routes are shown: one that follows the thermalization curve of Fig. 2 (shown dashed), and one that departs from this curve according to the anti-thermalization picture outlined in Section 3.2.

with the factor δ which applies for suprathermal particles). This should illustrate the possible differences from the case of post-shock thermalization. We consider an initially thermalized gas with parameters T_0, R_0, Γ_0 and obtain the $\Gamma - R$ relation

$$(\Gamma - 1)(R - 1) = \frac{kT_0}{\beta m^*} + \frac{1}{3}\left(\beta - \frac{1}{\beta}\right)R_0, \tag{41}$$

where $R = \beta R_0$ and m^* is the mean rest mass of the particles in the plasma. This picture of the processes at work in a collisionless shock front is almost certainly unrealistic, but it gives us a useful guide to the differences which may arise if the assumption of thermalization is relaxed.

Thus, given initially thermalized material whose state is specified by some point on the $\Gamma - R$ curve in Fig. 3, we can derive two possible thermodynamic paths for the shocked material, one which continues along the thermalization curve and one which departs from it. This behaviour is illustrated in Fig. 4 for a variety of starting points. In principle, the two most extreme ways in which the energy in the bulk fluid may be divided are that all the energy is given either to the electrons or to the protons and other nuclei. However, the cases of thermalization or the 'anti-thermalization' picture outlined above are already sufficiently extreme for the $\Gamma - R$ curves expected for the most extreme energy partitions to be quite similar to those in Fig. 4. Hence, we shall generally consider the alternatives of thermalization or anti-thermalization to give an indication of the extremes within which the value of Γ_2 might lie.

3.3 VELOCITIES AND SPECTRAL INDICES

We are now in a position to derive the propagation relations for any shock, given an assumption about Γ_1 and the degree of thermalization behind the shock. These are shown in Fig. 5

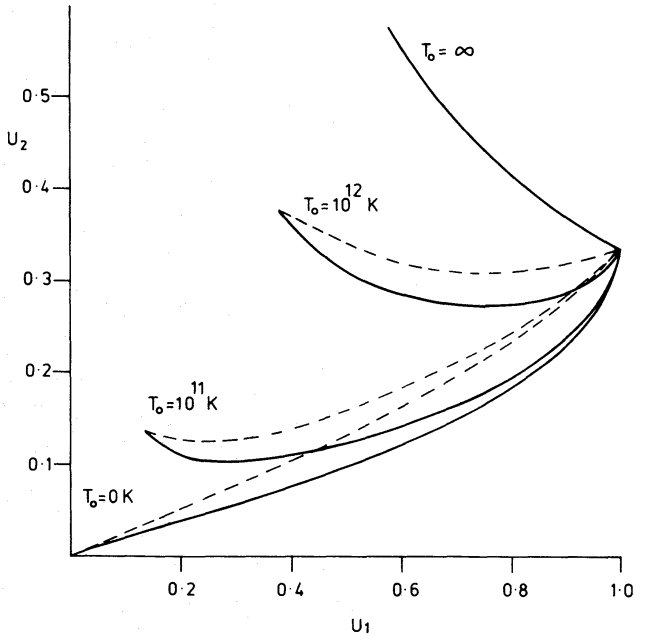

Figure 5. The shock propagation relation u_2 versus u_1, plotted for four initial temperatures of the unshocked material: 0, 10^{11}, 10^{12}K and ∞. For each case, a pair of curves is drawn – the solid one corresponding to the case of post-shock thermalization, the dashed one corresponding to the case of post-shock anti-thermalization (see Section 3.2).

as plots of u_2 versus u_1, for a variety of temperatures of the unshocked material. As the shocks become weaker, $u_2 \rightarrow u_1$, and $u_2 = u_1$ at the sound speed corresponding to Γ_1; the maximum possible value of u_2 is $1/\sqrt{3}$ for a weak shock in very hot ($\Gamma_1 = 4/3$) matter. As the strength of the shock increases, in all cases, $u_2 \rightarrow 1/3$ and $u_1 \rightarrow 1$. Thus, we see that the post-shock flow may never become highly relativistic, thereby justifying the arguments used to obtain $P(\phi)$ in Section 2.4.

To use the velocity curves in Fig. 5 to obtain spectral indices, we must now return to the problem of determining the distributions of θ_1 and θ_2 for particles crossing the shock. A first approach is to assume that these are given simply by the limiting forms at large distances upstream and downstream. The spectral indices that result from this assumption are shown in Fig. 6(a), plotted against u_1. We see that consideration of shock waves with a wide range of propagation speeds, rather than only those with speeds much less than c, complicates the situation in that any positive spectral index may now be produced, rather than the 'universal' spectral index of 0.5 produced by slow shocks. The differences from the simple non-relativistic strong shock case become more extreme as the temperature of the unshocked material is raised. For cold matter, we obtain $\alpha = 0.5$ as $u_1 \rightarrow 0$, but α falls as u_1^+ increases. This is due to two effects: (i) the nature of the acceleration process and (ii) the change in the shock compression ratio as the shock becomes stronger. The first point arises due to the fact that the post-shock flow never becomes highly relativistic; $\langle P \rangle$ therefore remains large (> 0.2) even for ultrarelativistic shocks, whereas δ increases without limit as $u_1 \rightarrow 1$, causing α to tend to 0 as $u_1 \rightarrow 1$. However, this effect is only important when the shock becomes ultrarelativistic: for $u_1 \lesssim 0.8$, the spectral indices produced for a constant compression ratio remain relatively constant. The second effect is due to the heating of the bulk material by the shock; at some point Γ_2 changes from 5/3 to 4/3, causing the compression ratio to change from 4 to 7, thus increasing δ and reducing α. The velocity at which this occurs depends on the equation of state: if the post-shock material is thermalized, then the

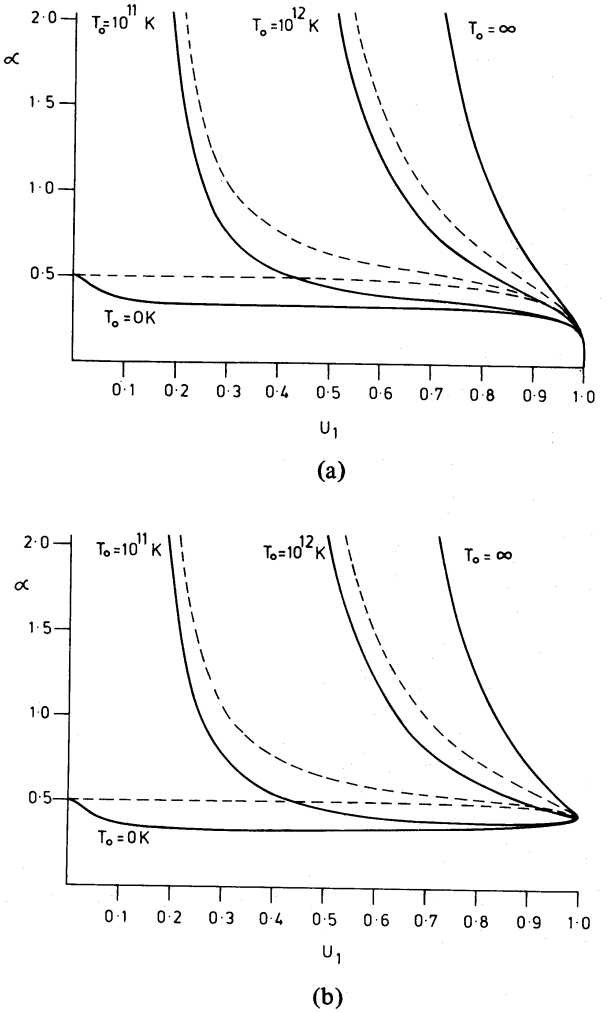

Figure 6. The spectral indices produced by Fermi acceleration in the shocks whose propagation relations are shown in Fig. 5, assuming the distributions of ϕ for particles crossing the shock to be given by (a) equations (15) and (17) and (b) equation (17) only.

bulk electrons become relativistic at $u_1 \simeq 0.1$ and the spectral index produced then remains at about 0.3 for $0.1 \lesssim u_1 \lesssim 0.9$.

Similar effects are found for shocks in hot material, except that the shocks are now weak for propagation velocities near to the sound speed. This means that $\Delta \to 0$ while u_2 remains high enough that all particles escape essentially without acceleration, leading to very large values of α. In this case, since no acceleration is occurring, the shape of the cosmic-ray spectrum will be dominated by the form of the injection spectrum. In practice, particles may well be processed by several shocks and it is the flattest spectrum which will prevail.

Finally, we must consider the effect on α of the uncertainties in the distributions of θ_1 and θ_2 crossing the shock; we have stated in Section 2.2 that these distributions should be some form intermediate between those of equations (15) and (17). This uncertainty is unlikely to make a significant change in $\langle P \rangle$: we have seen in Section 2.4 that $P(\phi)$ does not vary greatly with ϕ, even for the strongest shocks. The variations in δ, however, can be large: for a highly relativistic shock with $u_1 \simeq 1$ and $u_2 = 1/3$, $(1 + \Delta\cos\theta_1)$ can vary between 0 and 2, whereas $(1 + \Delta\cos\theta_2)$ can vary only between 4/3 and 2. Hence, although the changes to $\log\delta$ caused by uncertainties in the distribution of θ_2 are small, uncertainties in the distribution of θ_1 can make major changes to α if $\cos\theta_1$ is forced to take values close to $-u_1$. To investigate this

possibility, we evaluated α in the case where the distribution of particles crossing from the upstream side has the form characteristic of the downstream particles (equation 17). In this case, the distribution throughout the downstream region obviously has the same form, so that specifying the distribution of θ_1 fixes the distribution of θ_2. The spectral indices produced in this situation are shown in Fig. 6(b). The differences between Fig. 6(a) and (b) are small for $u_1 \lesssim 0.8$, but there is a great difference for larger velocities: in Fig. 6(b) $\alpha \rightarrow 0.43$ as $u_1 \rightarrow 1$, rather than tending to 0 as in Fig. 6(a). This is due to the point discussed above; the assumption of the form (17) for the distribution of particles crossing from the upstream region forces $\cos\phi$ to take values near to $-u_1$ as $u_1 \rightarrow 1$, thus reducing δ and steepening the spectrum. However, this case is something of an extreme: the mixing at the boundary will make the upstream angular distribution become closer to (17), but will never cause equality with (17) to be achieved. Hence, for the model of the scattering assumed here, the true answer should lie somewhere between Fig. 6(a) and (b).

The one remaining uncertainty in this analysis is the effect of different models for the scattering process. We have seen that the forms of $P(\phi)$ and of the downstream angular distribution should be reasonably model-independent; the only possible variation is therefore in the upstream angular distribution (equation 15). Although it is difficult to assess exactly how large this variation could be, it is unlikely to be important; Fig. 6(a) and (b) show that changing the assumed form of the upstream angular distribution from (15) to (17) makes a negligible difference to α for $u_1 \lesssim 0.8$. Although different models for the upstream scattering will yield different angular distributions, it is most unlikely that any such changes could be significantly more extreme than the difference between (15) and (17). Thus, changes to α due to uncertainties in the distribution of θ_1 are likely to be small for $u_1 \lesssim 0.8$. For higher velocities α can vary considerably, but in fact such ultrarelativistic shocks will probably not be capable of accelerating particles in the observable range of energies (see Section 4.2). Hence we conclude that Fig. 6(a) and (b) should give a reasonably accurate picture of the spectral indices produced by Fermi acceleration in relativistic shock waves. The most important point is that, for strong shocks, the spectral index remains small – in the range 0.3 to 0.5 – for a wide range of velocities.

4 Application of the mechanism in practice

4.1 INJECTION

So far, we have not found it necessary to consider precisely where suprathermal particles are injected into the acceleration mechanism. If, in fact, turbulent plasma mechanisms are the most likely sources of injected particles, then we expect the downstream region to be the site of injection (Blandford & Rees 1974). The spectrum of the Fermi-accelerated particles is, however, independent of the site of injection. Similarly, time variations in injection will not affect the spectrum, provided that there is no variation on time-scales comparable with that necessary for the establishment of the spectrum. This is characterized by the typical time-scale for a particle to complete one cycle of crossing and re-crossing the shock, namely $\sim D/u_2^2$, where D is the post-shock diffusion coefficient (Blandford 1979). The spectrum is obviously unaffected if the injection averaged over this time-scale is relatively constant, so that neither slow systematic changes nor fast fluctuations in injection will change the spectrum.

An extremely important point concerning the application of this mechanism in practice is the rate of injection. The acceleration mechanism itself is very efficient, but the rate of production of ultrarelativistic particles is limited by the rate at which mildly suprathermal particles are injected. From this point of view, strong shocks will be more important than weak ones if we assume that a certain fraction of the total turbulent energy in the downstream

region is channelled into suprathermal particles (Blandford & Rees 1974). Hence the very steepest spectra in Fig. 5 are probably not important, as the corresponding shocks are very weak and will have a low injection rate.

4.2 THE THRESHOLD ENERGY

We have until now assumed that a sufficiently energetic particle will penetrate the shock front undeviated, without quantifying this statement. The energy which is necessary (the threshold energy) depends on the processes at work in the collisionless shock front, which are uncertain. The picture we have is of a region of turbulent electromagnetic fields which randomize the incident bulk flow, leading to compression. For a thermal particle of mass m and charge q, incident at u_1, the impulse received per unit charge, $d\pi_q$, is given by

$$d\pi_q \sim \pi/q = \frac{\gamma_1 m u_1}{q} . \tag{42}$$

For a suprathermal electron to cross the shock front undeviated we require $d\pi_e \ll \pi_e$, where

$$\pi_e = \frac{\gamma_e m_e}{q_e} .$$

However, if the shock is capable of randomizing the incident He nuclei, then, since for these

$$d\pi_\alpha = \frac{2\gamma_1 m_p u_1}{q_e} ,$$

the above condition becomes

$$\gamma_e \gg 2\gamma_1 \frac{m_p}{m_e} u_1 , \tag{43}$$

and very high electron energies (~ 2 GeV for a mildly relativistic shock with $u_1 \simeq 1$ and $\gamma_1 \simeq 1$, corresponding to $\gamma_e = 4000$) are required before acceleration is possible. It is interesting to place this in the context of radio observations by considering the best-studied region of an extragalactic source where particle acceleration is thought to occur, namely the hot-spots of Cyg A. Here, the standard assumption of equipartition yields magnetic fields of 40 nT (Hargrave & Ryle 1976). The emissive maximum of electrons with a Lorentz factor γ is at a frequency of $0.44\gamma^2 q_e B/2\pi m_e$ (Pacholczyk 1970) which, for $\gamma = 4000$, corresponds to a frequency of 8 GHz. Hence, on this picture, acceleration by a highly relativistic shock would not be important in the normal range of radio observations (10 MHz–15 GHz), although for a shock with $u_1 = 0.1$ the critical frequency would be reduced to 80 MHz and acceleration would be important, as it would also in the 'tails' of Cyg A, where the magnetic field is much weaker than in the hot-spots, and the critical frequency is correspondingly lower by a factor of 10–1000. These figures do not apply for an ultrarelativistic shock, where the threshold energy is increased by a factor γ_1. The most highly relativistic shocks are therefore unlikely to be capable of accelerating particles in the observable region, so the uncertainties in α at large u_1 discussed in Section 3.3 are not important.

4.3 COMPLICATIONS TO THE SHOCK PROPAGATION

There remains the possibility that the u_2 versus u_1 relations in Section 3.3 may require modification.

We have solved the shock equations by assuming a perfect gas, without taking account of the magnetic field. Magnetohydrodynamic shocks were considered by de Hoffmann & Teller (1950), who found two simple cases:

(i) If the shock propagates parallel to a magnetic field, then the shock equations (27)–(29) are unchanged.

(ii) If the propagation is perpendicular to the field, then the effect is to compress the field so that $B_2/B_1 = \rho_2/\rho_1$ and to add a term $B^2/2\mu_0$ to P and e on either side of the shock. The shock is consequently made less strong and α will increase. This second case, however, cannot lead to acceleration as there is no possibility of diffusion away from the shock; the particles will be carried through with the field lines and have their energies increased by some finite factor. In reality, the pre-shock magnetic field will probably be random and diffusion will be allowed, although the magnetic field will be dynamically important if it is sufficiently strong.

There is also the objection that throughout we have considered the suprathermal particles to be a dynamically negligible perturbation to the shock. Blandford (1980) considers the possibility that this is not so and that the cosmic ray pressure may become significant. By means of a perturbation argument, he shows that the spectrum may either steepen or flatten by amounts of order P_{cr}/P_{ram}, where P_{ram} is the ram pressure of the incoming material.

Both of these modifications may indeed be relevant in hot-spots, since simple pressure-balance arguments show that $P_{cr} = P_{ram}$ and, assuming equipartition, $e_{mag} \sim e_{cr}$. The problem is almost certainly more complex than this, due to its three-dimensional nature – the cosmic-ray density and magnetic field within the emitting region which we call a hot-spot do not necessarily have the same values at the shocks which bound the whole system. It is clear that much further study of this problem is necessary.

5 Conclusions

The acceleration of charged particles by relativistic shock waves has been investigated for differing physical conditions. For strong shocks, a synchrotron spectral index in the range 0.3–0.5 is produced for a wide range of propagation velocities. There is some uncertainty in α for highly relativistic shocks, but the threshold energy in such cases is probably too high for the acceleration mechanism to operate. Thus, it seems that very steep spectra may be produced only by weak shock waves in hot material.

These conclusions are very relevant to the powerful extragalactic radio sources, where the observed range of α is $0.5 \lesssim \alpha \lesssim 2.0$. Attempts to explain the variation of spectral indices found in the extragalactic sources have often considered the steepening effects of synchrotron losses on an injection spectrum with $\alpha = 0.5$. However, although a spectral index of around 0.5 arises from strong shocks for a wide range of physical conditions, the value is generally < 0.5. Since, in the steady-state, synchrotron losses can produce an increase of only 0.5 in α, aging effects are unable to account for the steepest spectra, and the weak shocks in hot material may be of astrophysical significance in this context.

Acknowledgments

It is a pleasure to thank S. F. Gull and P. A. G. Scheuer for many fruitful discussions on the subject of particle acceleration. I am extremely grateful to a referee for pointing out some shortcomings with the original version of this paper. I also thank the SRC and the Cavendish Laboratory for financial support.

References

Abramowitz, M. & Stegun, I. E., 1965. *Handbook of Mathematical Functions,* Dover, New York.

Axford, W. I., Leer, E. & Skadron, G., 1977. *Proc. 15th International Conference on Cosmic Rays,* Plovdiv, Bulgaria.

Bell, A. R., 1978a. *Mon. Not. R. astr. Soc.,* **182,** 147.

Bell, A. R., 1978b. *Mon. Not. R. astr. Soc.,* **182,** 443.

Blandford, R. D., 1979. *Particle Acceleration Mechanisms in Astrophysics,* A.I.P. Conf. Proc. No. 56, p. 333.

Blandford, R. D., 1980. *Astrophys. J.,* **238,** 410.

Blandford, R. D. & McKee, C. F., 1976. *Phys. Fluids,* **19,** 1130.

Blandford, R. D. & Ostriker, J. P., 1978. *Astrophys. J.,* **221,** L229.

Blandford, R. D. & Ostriker, J. P., 1980. *Astrophys. J.,* **237,** 793.

Blandford, R. D. & Rees, M. J., 1974. *Mon. Not. R. astr. Soc.,* **169,** 395.

Chandrasekhar, S., 1939. *An Introduction to the Study of Stellar Structure,* Chicago University Press.

Cox, D. R. & Miller, H. D., 1965. *The Theory of Stochastic Processes,* Methuen, London.

de Hoffmann, F. & Teller, E., 1950. *Phys. Rev.,* **80,** 692.

Hargrave, P. J. & Ryle, M., 1976. *Mon. Not. R. astr. Soc.,* **175,** 481.

Landau, L. D. & Lifshitz, E. M., 1959. *Fluid Mechanics,* Pergamon, Oxford.

Longair, M. S. & Riley, J. M., 1979. *Mon. Not. R. astr. Soc.,* **188,** 625.

Pacholczyk, A. G., 1970. *Radio Astrophysics,* W. H. Freeman, New York.

Parker, E. N., 1976. *The Physics of Non-Thermal Radio Sources,* p. 169, D. Reidel, Dordrecht, Holland.

Scheuer, P. A. G. & Readhead, A. C. S., 1979. *Nature,* **277,** 182.